Strength and stiffness anisotropy of 3-D printed coarse root analogues for small-scale physical modelling

Author 1

- Raul Batista Araujo de Sousa, MSc, Postgraduate student
- Department of Civil and Environmental Engineering, the Hong Kong University of Science and Technology, Hong Kong, SAR, China
- E-mail: rbads@connect.ust.hk
- ORCID number: 0000-0001-8124-2420

Author 2 (corresponding author)

- Anthony Kwan Leung, PhD, Associate Professor
- Department of Civil and Environmental Engineering, the Hong Kong University of Science and Technology, Hong Kong, SAR, China
- E-mail: ceanthony@ust.hk
- ORCID number: 0000-0002-5192-5033

Author 3

- Jonathan Adam Knappett, PhD, Professor of Civil Engineering
- School of Science and Engineering, University of Dundee, UK
- E-mail: j.a.knappett@dundee.ac.uk
- ORCID number: 0000-0003-1936-881X

Author 4

- Xingyu Zhang, PhD, Lecturer

- Department of Civil and Airport Engineering, Nanjing University of Aeronautics and Astronautics, Liyang, China
- E-mail: x.y.zhang@nuaa.edu.cn
- ORCID number: 0000-0002-7697-9871

Date of text written: 06/02/24

Number of words in main text: 2164

Number of figures: 5

This is the accepted manuscript for: de Sousa, RBA, Leung, AK, Knappett, JA & Zhang, X 2024, 'Strength and stiffness anisotropy of 3-D printed coarse root analogues for small-scale physical modelling', Geotechnique Letters, vol. 14, no. 4, pp. 1-6. https://doi.org/10.1680/jgele.23.00087

Abstract

Plant root–soil mechanical interaction in the application of soil bioengineering such as tree and slope stability has been investigated via centrifuge modelling, utilising root analogues to replicate vegetated soils. Three-dimensional (3-D) printing can be used to model complex root architecture, but the nature of the layer-upon-layer printing process may lead to printed parts of differing tensile behaviour depending on orientation and, consequently, unrealistic simulation of root mechanical reinforcement. This study aimed to assess the strength and stiffness anisotropy of straight root analogues built at varying orientations via three different 3-D printing methods and compare the measured properties with those of real roots. The tensile strength ratios between horizontally- and vertically-printed samples were up to 3.90, 1.27 and 2.57 for fused deposition modelling (FDM), liquid-crystal display (LCD) and Polyjet methods, respectively. Stiffness anisotropy was also more significant in FDM. The relatively higher anisotropy in FDM-printed samples could overestimate the strength and stiffness of most roots in a hypothetical heart-shaped root system, depending on the diameter distribution. Such a physical model may be improved using 45° inclined Polyjet-printed rods.

Keywords: Models (physical); Centrifuge modelling; Tensile properties; Vegetation; UN SDG 11.

1. Introduction

The mechanical interactions between coarse tree roots and soil can be relevant for understanding the tree anchorage behaviour (Zhang et al., 2020) and the stability of forested slopes during tree clean-cut and reforestation schemes (Stokes et al., 2009) (Figure 1(a)). That is because coarse roots might dominate the root reinforcement at the tree scale (Giadrossich et al., 2019), although the effectiveness of such reinforcement would depend on site-related factors such as external loads (e.g., windstorms and tree surcharge), slope gradient and mode of potential failure (Nilaweera and Nutalaya, 1999). The complexities of rooted soils can be revealed by empirically observing the interplay between roots and soil, which is principally led by the mobilisation of root-soil frictional and root tensile properties (Mickovski et al., 2007). However, the practical difficulties in obtaining spatial and mechanical properties of large-sized root (diameter > 10 mm) traits in the field (Reubens et al., 2017) and at laboratory scale (Giadrossich et al., 2017) impose challenges on the study of the reinforcing effects of this class of roots. In this context, small-scale modelling via centrifuge provides a more straightforward way to study vegetated soils by scaling down the dimensions of large roots while keeping field-representative soil stresses under controllable boundary conditions (Liang et al., 2015). Early studies have employed small-scaled root analogues of highly simplified architecture (Sonnenberg, 2012; Kamchoon et al., 2014). Later, Liang et al. (2015) introduced root analogues manufactured by three-dimensional (3-D) printing which could produce much more complex and realistic architecture. However, the nature of the layer-upon-layer printing process might lead to printed parts of differing tensile behavior in different directions (Yao et al., 2019). The build orientation (i.e., orientation at which the part is positioned relative to the three major axes of the 3D printer) might influence the failure mechanism and the level at which stress is being transferred along the printed part (Eryildiz, 2021). Given the bonding between adjacent print layers is typically weaker than the print material's intrinsic strength,

parts with layers printed parallel to the direction of soil shear (i.e., perpendicular to the primary tensile stress acting on the printed root part) may be weaker in that direction. Conversely, parts with layers perpendicular to the shear stress direction (i.e., parallel to the primary tensile stress direction) may be stronger (Figure 1(b)) (Uddin et al., 2017). This could produce unrealistic mobilisation of stresses during root analogue breakage, leading to questionable test data when being used to benchmark and evaluate the accuracy and reliability of root-soil interaction models (e.g. Zhu et al., 2022).

This study investigates the anisotropy of the tensile properties of 3-D printed root analogues produced by three different printing methods, namely fused deposition modelling (FDM), liquid-crystal display (LCD) and Polyjet, that are all relevant to producing complex root architecture system for physical model tests. How the tensile behavior of the printed models affects the selection of the printing method for producing root analogues for physical modelling is discussed.

2. Materials and methods

2.1. 3D printing

Three 3-D printing methods were tested in this study (Figure 1(c)). FDM is a material extrusion-type process that works by heating a thermoplastic material to a semi-liquid state and depositing it in layers along the extrusion path (Ahn et al., 2002). LCD is a type of vat polymerisation where an ultraviolet (UV) light is emitted through a pattern displayed by an LCD screen to selectively cure a liquid photopolymer resin layer by layer (Mele and Campana, 2022). Polyjet is a material jetting technique that operates by pouring tiny droplets of photosensitive resin that are immediately UV cured, solidified, and built on the previous layer (Lumpe et al., 2019). Table 1 summarises the relevant specifications of the printer, material, and printing process for each method.

Cylindrical rods of 160 mm in length and diameters varying from 1.5 to 6 mm were printed at horizontal (H), vertical (V) and 45° inclined (I) orientations for each method. The cylindrical shape was selected to mimic typical root traits used in tensile tests (Wu et al., 2021). The diameter range covers a realistic range for coarse tree roots; considering a model scaling factor of as small as, say 1:10, the analogues would be replicating roots with prototype diameters ranging from 15 mm to 60 mm, which is representative to small-size trees. The rod orientations represent dominant traits in three main types of root systems (Kostler et al., 1968), that is: lateral roots in a plate system, tap root in a taproot system, and oblique roots in a heart-shaped system (Figure 2). Although all 3-D printers could technically produce rods of less than 1.5 mm in diameter, the thin nature of the relatively long printed rod would lead to undesirable instability during the printing process of non-horizontal models. This way, vertical and/or inclined samples with diameters less than 2 mm (even 3 mm for FDM) could not be properly printed without imperfections and were therefore discarded.

2.2. Tensile tests

Uniaxial tensile tests were conducted in triplicate with an EZ-50 universal testing machine (wedge tensile grips, 1kN load capacity, 5 mm/min loading rate). Rods that had a 100 mm gauge length were reinforced at the ends with epoxy resin to prevent sample damage and sandpaper to avoid slippage. A test was valid once breakage happened within the gauge length. These procedures accorded to the common protocols for conducting root tensile tests (Giadrossich et al., 2017).

3. Results and discussion

3.1. Tensile behaviour of 3-D printed models

Horizontal rods printed via FDM presented average tensile strength (TS, i.e., tensile stress at breakage) that reduced with diameter (Figure 3(a)). Previous studies (Liang et al., 2015; Zhang et al., 2020) considered such a trend as propitious for mimicking the commonly reported negative correlation between TS and diameter in real roots (e.g., Wu et al. 2021), but this relationship was not as clear for inclined and vertically-printed samples. The TS of the horizontally-printed samples was up to 3.9 and 2.5 times higher than that of the vertically- and inclined-printed ones, respectively. A small TS discrepancy (TS ratio, i.e., ratio between the TS values of horizontally- and inclined/vertically-printed samples, < 1.5) was observed only between a few inclined and horizontally-printed samples (Figure 3(b)), highlighting a significant strength anisotropy due to printing orientation. For LCD printed samples, there was no significant discrepancy among the three different build orientations (Figure 3(c)) as the values of TS ratio were all less than 1.5 (Figure 3(d)). The TS of Polyjet printed samples increased with diameter in all build orientations (Figure 3(e)). This could be due to printing imperfections along the surface of thinner rods, which might cause weak spots that would lead to stress concentration and thus lower TS. As the sample diameter increased, the influence of such imperfections became less significant as compared to the overall sample size. The TS of horizontally-printed samples were up to 2.57 and 1.43 times larger than that of vertically- and inclined-printed ones, respectively (Figure 3(f)). The higher strength anisotropy found in the FDM printed samples, when compared with other printing methods, suggests poorer interlayer bonding that leads to relatively lower strength in non-horizontal parts.

Much larger stiffness anisotropy was found for the FDM printed samples (Figure 4(a) and 4(b)) when compared with the LCD and Polyjet methods. The latter two produced elastic

153 modulus (EM, i.e., gradient of the initial linear portion of a tensile stress-strain curve up to a
154 strain of 0.02 for the horizontally- and inclined printed samples and 0.01 for the vertically-
155 printed samples) ratios between the horizontally- and vertically-printed samples up to 1.8 and
156 1.17, respectively (Figure 4(c) – 4(f)). Although the presence of strength and stiffness anisot-
157 ropy tends to make horizontally-printed root analogues to have a higher strength and stiff-
158 ness, this would mainly affect the root–soil mechanical interaction for analogues that tend to
159 fail by breakage. In this case, under the same loading condition and considering that the prop-
160 erties of horizontally-printed root analogues are representative of real roots, the analogues
161 that are printed vertically and inclined would mobilise less strength, which is not what neces-
162 sarily would happen in real condition. Otherwise, in a scenario where root breakage is not
163 supposed to happen, the smaller TS values of vertically-printed samples would not impose a
164 problem, so printing technologies that create anisotropic properties (i.e., FDM) could still be
165 used.
166
167 Most values of TS (Figure 3) and EM (Figure 4) were out of the range provided by the manu-
168 facturer for all three printing methods. The discrepancies can be due to the different condi-
169 tions at which samples were produced and the tensile tests were performed. The printing pa-
170 rameters reported by the manufacturers to print standard flat-dog-bone samples for tensile
171 tests might not be the most suitable ones for printing more complex structures, so a trial-and-
172 error exercise is usually performed and these parameters can be changed according to the
173 user's relevant criteria (e.g., design accuracy, printing time, material cost). Once the set of pa-
174 rameters for printing the root analogue is defined, conducting tensile tests considering the
175 case-specific conditions produces results that better reflect the mechanical behaviour of the
176 printed parts.
177

3.2. 3D printed models to represent real roots in physical modelling tests

To compare the mechanical behaviour of printed root traits to those from real roots, the mechanical properties of inclined printed rods were chosen to represent the heart-shaped root system (i.e., oblique root system), which is a common shape for tree roots grown on slopes (Kozlowski, 1971). Although it did not produce the most mechanically isotropic traits as compared to LCD, Polyjet method was selected given the printer's larger build volume (Table 1) and capacity of using a soluble material as the support, which eliminates the risk of breaking the parts as in traditional support removal (i.e., trimming), and reduces post-processing time and effort.

Figure 5 shows the upper and lower bounds for TS and EM of tree roots collected from the literature (Tables S1 and S2 in supplementary information). As very few data are available for root diameters larger than 10 mm, these bounds were considered the references for assuming constant values of TS and EM for thicker roots. Indeed, a diameter-independent range of mechanical properties are commonly considered for stem wood (Kretschmann, 2010), so the same was assumed for coarse roots (D> 10 mm), as they are also made of secondary xylem fibers (i.e., wood) (Pratt et al., 2007). A hypothetical scaling factor of 15 was considered for small scale (1:N) modelling in centrifuge, where the rods would be simulating prototype roots of length dimensions 15 times larger, whilst maintaining the same prototype's mechanical properties (Figures 5(a) and 5(b)). The values of TS of the 45° inclined printed Polyjet rods were within the range for tree roots at diameters up to 45 mm in prototype, but still relatively closer to this range for bigger diameters as compared to linden wood, which was used to simulate woody roots (i.e., coarse roots) in non-printed models by Sonnenberg et al. (2012). The FDM printed ABS rods produced by Liang et al. (2015) also had TS values partially within the assumed range (Figure 5(a)). However, it is worth noting that these rods were printed at

horizontal orientation. Given the significant TS and EM anisotropy by the FDM printing method (Figures 3 and 4), the properties of roots within the hypothetical heart root system may drop closer to (or even further) within the range of real tree roots due to the reducing trend of the TS ratio with diameter. The EM of the Polyjet rods were less representative than the TS, but still closer to the assumed root values than the stiff analogues made of linden wood (Figure 5(b)). For 1-***g*** physical modelling at 1:1 scale (where the same length and mechanical properties between model and prototype are maintained), all the values of TS of inclined Polyjet rods were within the assumed TS range (Figure 5(c)), yet not the case for EM (Figure 5(d)).

4. Conclusions

3-D printed root analogues for geotechnical physical modelling present a certain degree of strength and stiffness anisotropy induced by build orientation regardless of the printing method used. Test results reveal that such anisotropy was higher using the FDM printing method, followed by the Polyjet and LCD methods, the latter of which were close to isotropic in both strength and stiffness. Using the measured tensile properties of printed parts that better represent the whole root system would prevent significant overestimation or underestimation of the mechanical behaviour of root analogues in model tests. The values of TS and EM of 45° inclined Polyjet rods had a relatively good agreement with those of real roots and could be considered for modelling the behavior of small-scaled heart-shaped tree root systems in 1:N centrifuge or 1-***g*** tests. In summary, considering the effect of build orientation when 3-D printing load-bearing root parts is essential to ensure the model provides a representative (but still not an exact physical twin of) prototype, for interpreting results from model tests and for simulating either 1***g*** or high-***g*** model properties in validating numerical simulations.

Acknowledgements

The authors thank the Hong Kong Research Grant Council (Grant Nos. GRF/16202422 and CRF/C6006-20G), the National Natural Science Foundation of China (Grant No. 51922112) and the Natural Science Foundation of Jiangsu Province (Grants No. BK20230895) for the funding and the resources spent on this work.

References

Ahn, S. H., Montero, M., Odell, D., Roundy, S., & Wright, P. K. (2002). Anisotropic material properties of fused deposition modeling ABS. *Rapid prototyping journal*, *8*(4), 248-257.

Eryildiz, M. (2021). Effect of build orientation on mechanical behaviour and build time of FDM 3D-printed PLA parts: an experimental investigation. *European Mechanical Science*, *5*(3), 116-120.

Giadrossich, F., Cohen, D., Schwarz, M., Ganga, A., Marrosu, R., Pirastru, M., & Capra, G. F. (2019). Large roots dominate the contribution of trees to slope stability. *Earth Surface Processes and Landforms, 44*(8), 1602-1609.

Giadrossich, F., Schwarz, M., Cohen, D., Cislaghi, A., Vergani, C., Hubble, T., ... & Stokes, A. (2017). Methods to measure the mechanical behaviour of tree roots: a review. *Ecological engineering*, *109*, 256-271.

Kamchoom, V., Leung, A. K., & Ng, C. W. W. (2014). Effects of root geometry and transpiration on pull-out resistance. *Géotechnique Letters*, *4*(4), 330-336.

Köstler, J. N., Brückner, E., & Bibelriether, H. (1968). Die Wurzeln der Waldbäume: Untersuchungen zur Morphologie der Waldbäume in Mitteleuropa. *(No Title)*.

Kozlowski, T. T. (1971). Growth and development of trees. Volume II. Cambial growth, root growth, and reproduction growth. *Growth and development of trees. Volume II. Cambial growth, root growth, and reproduction growth.*

Kretschmann, D. (2010). Mechanical properties of wood. *Wood handbook: wood as an engineering material: chapter 5. Centennial ed. General technical report FPL; GTR-190. Madison, WI: US Dept. of Agriculture, Forest Service, Forest Products Laboratory, 2010: p. 5.1-5.46.*, *190*, 5-1.

Liang, T., Knappett, J. A., & Duckett, N. (2015). Modelling the seismic performance of rooted slopes from individual root–soil interaction to global slope behaviour. *Géotechnique*, *65*(12), 995-1009.

Lumpe, T. S., Mueller, J., & Shea, K. (2019). Tensile properties of multi-material interfaces in 3D printed parts. *Materials & Design*, *162*, 1-9.

Mele, M., & Campana, G. (2022). Advancing towards sustainability in liquid crystal display 3D printing via adaptive slicing. *Sustainable Production and Consumption*, *30*, 488-505.

Mickovski, S. B., Bengough, A. G., Bransby, M. F., Davies, M. C. R., Hallett, P. D., & Sonnenberg, R. (2007). Material stiffness, branching pattern and soil matric potential affect the pullout resistance of model root systems. *European Journal of soil science*, 58(6), 1471-1481

Nilaweera, N. S., & Nutalaya, P. (1999). Role of tree roots in slope stabilisation. *Bulletin of engi-neering geology and the environment, 57*, 337-342.

Pratt, R. B., Jacobsen, A. L., Ewers, F. W., & Davis, S. D. (2007). Relationships among xylem transport, biomechanics and storage in stems and roots of nine Rhamnaceae species of the California chaparral. *New phytologist*, *174*(4), 787-798.

Reubens, B., Poesen, J., Danjon, F., Geudens, G., & Muys, B. (2007). The role of fine and coarse roots in shallow slope stability and soil erosion control with a focus on root system architecture: a review. *Trees, 21*(4), 385-402.

Sonnenberg, R., Bransby, M. F., Bengough, A. G., Hallett, P. D., & Davies, M. C. R. (2012). Centrifuge modelling of soil slopes containing model plant roots. *Canadian Geotechnical Journal*, *49*(1), 1-17.

Stokes, A., Atger, C., Bengough, A. G., Fourcaud, T., & Sidle, R. C. (2009). Desirable plant root traits for protecting natural and engineered slopes against landslides. *Plant and soil*, *324*, 1-30.

Uddin, M. S., Sidek, M. F. R., Faizal, M. A., Ghomashchi, R., & Pramanik, A. (2017). Evaluating mechanical properties and failure mechanisms of fused deposition modeling acrylonitrile butadiene styrene parts. *Journal of Manufacturing Science and Engineering*, *139*(8), 081018.

Wu, Z., Leung, A. K., Boldrin, D., & Ganesan, S. P. (2021). Variability in root biomechanics of Chrysopogon zizanioides for soil eco-engineering solutions. *Science of The Total Environment*, *776*, 145943.

Yao, T., Deng, Z., Zhang, K., & Li, S. (2019). A method to predict the ultimate tensile strength of 3D printing polylactic acid (PLA) materials with different printing orientations. *Composites Part B: Engineering*, *163*, 393-402.

Zhang, X., Knappett, J. A., Leung, A. K., Ciantia, M. O., Liang, T., & Danjon, F. (2020). Small-scale modelling of root-soil interaction of trees under lateral loads. *Plant and Soil*, *456*(1), 289-305.

Zhu, J., Leung, A. K., & Wang, Y. (2022). Modelling root–soil mechanical interaction considering root pull-out and breakage failure modes. *Plant and Soil*, *480*(1-2), 675-701.

300 Table 1. Specification of the printer, material and parameters chosen for printing the models.

Specifications		Technology		
		FDM	LCD	Polyjet
Printer	Model	Bambu Lab X1 Carbon	Phrozen Sonic Mini 8K	J850 Prime
	Manufacturer	Bambu Lab	Phrozen Technology	Stratasys Ltd.
	Build volume	256 x 256 x 256 mm	165 x 72 x 180 mm	490 x 390 x 200 mm
	Accuracy[1]	+- 0.007 mm	+- 0.022 mm	+- 0.1-0.2 mm
	Min. layer width[2]	0.4 mm	0.01 mm	0.014 mm
Material	Name	ABS	ABS-like resin	Digital ABS (RGD515 + RGD531)
	Main composition (≥ 80%)	Acrylonitrile, butadiene, and styrene monomers	Acrylate monomer and epoxy diacrylate	Acrylic formulation (major components are proprietary)
	Tensile properties[4]	TS= 32-41 MPa EM=1.96-2.2 GPa	TS= 12 MPa EM= 0.95 GPa	TS=55-60 MPa EM=2.6-3 GPa
Relevant user-defined printing parameters		Layer height[3]: 0.15 mm; Infill density: 50%; Infill pattern: straight line; Printing speed: 100 mm/s; Support: same material (detach by trimming)	Layer height[3]: 0.05 mm; Exposure time: 2.5 s; Lifting distance: 6 mm; Lifting speed: 60 mm/min; Support: same material (detach by trimming)	Layer height[3]: 0.014 mm; Support: SUP706B (detach by dissolving with sodium hydroxide solution)

301 [1]Typical deviation from 3D model dimensions.
302 [2]Mininum feature size in the XY plane.
303 [3]Mininum feature size in the Z plane.
304 [4]Manufacturer provided values.
305
306
307
308
309
310
311
312

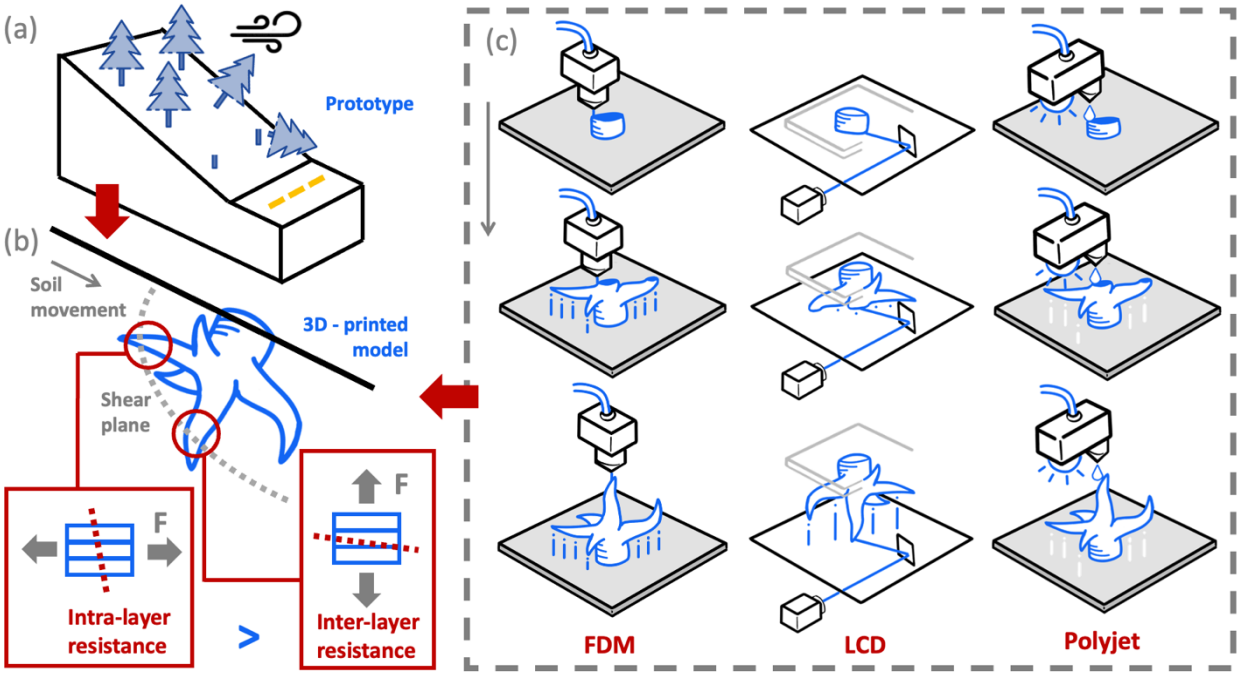

Figure 1. 3D printing for tree root modelling: (a) a vegetated slope under windstorm and clear-cutting, (b) a possible failure mechanism of vertically- and horizontally-printed root parts, (c) process of three 3-D printing methods.

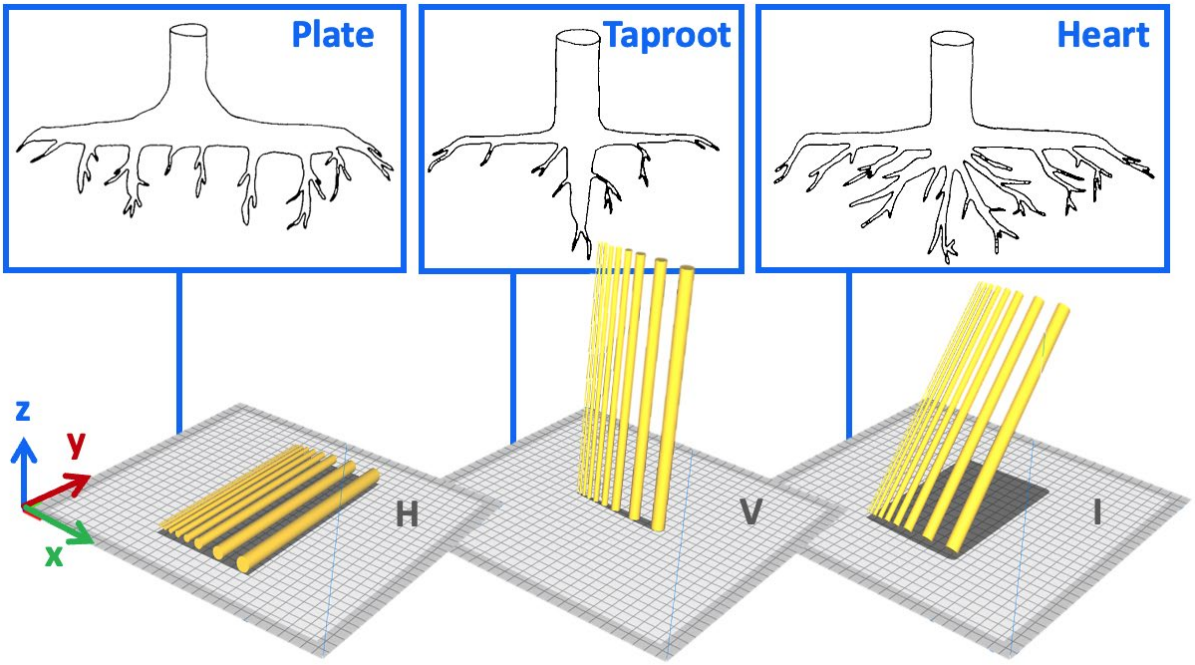

Figure 2. Rod orientations based on the main types of root systems (after Kostler et al., 1968).

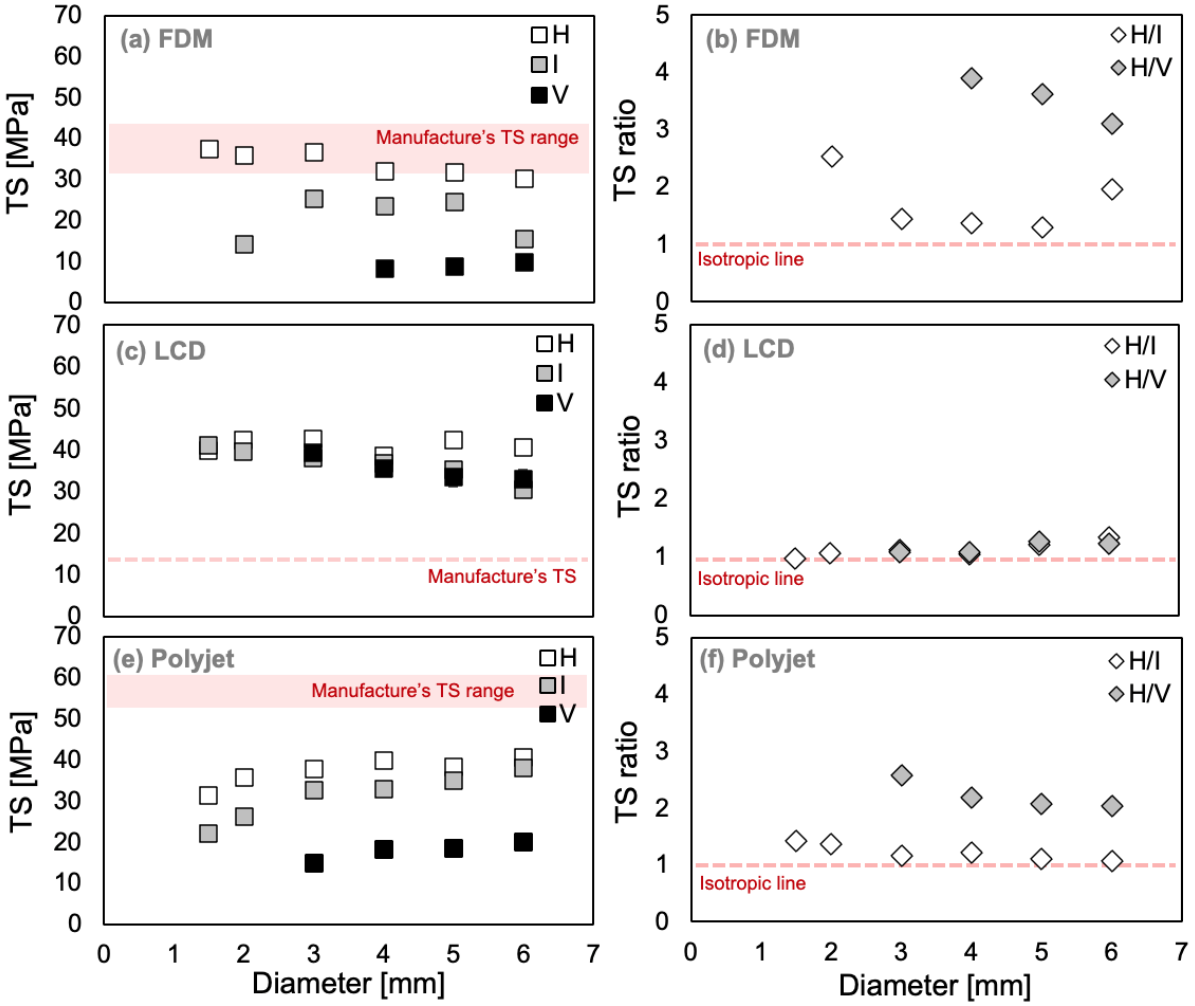

Figure 3. TS of the rods printed at different orientations and their respective ratios for: (a, b) FDM, (c, d) LCD, (e, f) Polyjet.

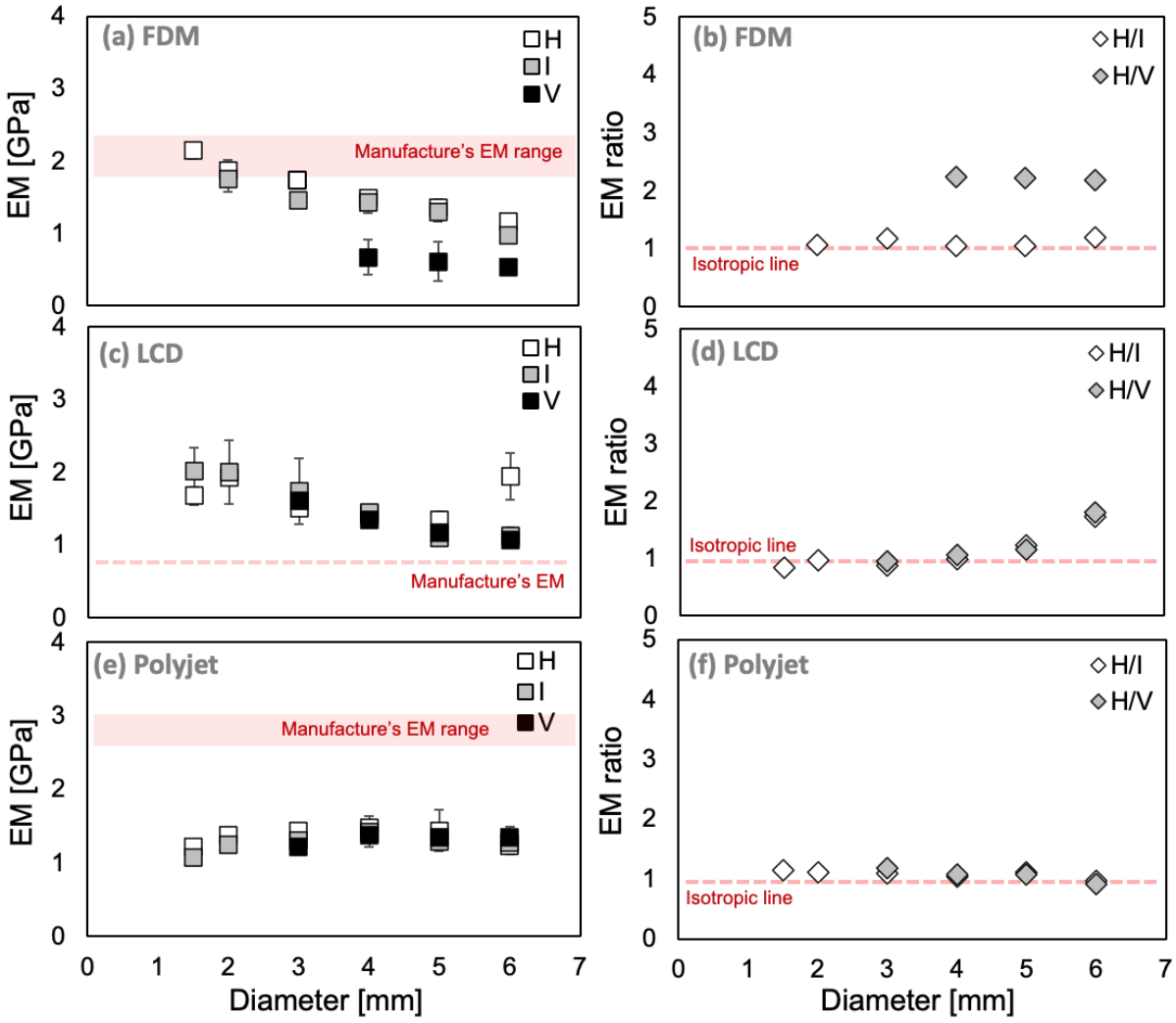

Figure 4. EM of the rods printed at different orientations and their respective ratios for: (a, b) FDM, (c, d) LCD, (e, f) Polyjet.

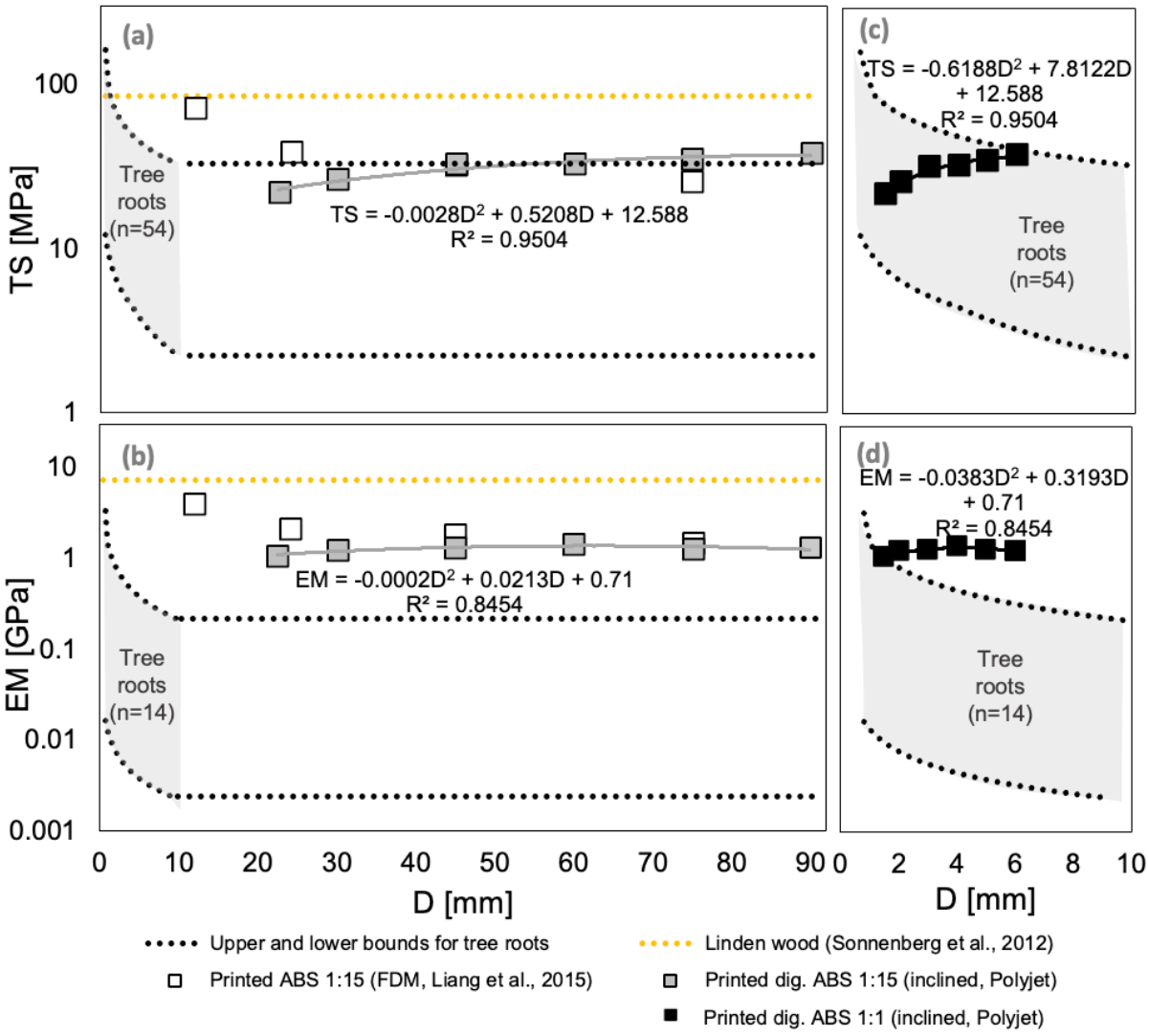

Figure 5. TS (a, c) and EM (b, d) of real roots (species and regression coefficients for TS and EM are shown in Tables 1S and 2S, respectively) and root analogues tested in the present study.